# EXPERIMENTAL VERIFICATION OF COMPRESSOR PERFORMANCE FOR AN ULTRA-MICRO GASTURBINE

**Jan Peirs*, T. Waumans, F. Al-Bender and D. Reynaerts**
Department of Mechanical Engineering, Katholieke Universiteit Leuven, Leuven, Belgium
*Presenting Author: jan.peirs@mech.kuleuven.be

**Abstract:** This paper presents the experimental verification of a 20 mm compressor prototype developed for a 1 kWe ultra-microgasturbine. The gasturbine has a nominal speed of 500 000 rpm, a nominal air flow of 20 g/s and a nominal pressure ratio of 3. Whereas the previous rotor was limited in speed to 261 000 rpm due to rotor instability, rotor dynamic modelling predicts that the new elongated rotor with externally damped air bearings remains stable up to 600 000 rpm, well beyond the nominal speed. Compressor maps are measured for speeds up to 240 000 rpm, and correspond well with the calculated characteristics.

**Keywords:** microturbine, air bearings, external damping, rotor dynamics, compressor map

## INTRODUCTION

This paper reports on the experimental verification of a 20 mm compressor prototype developed for a 1 kWe ultra-micro gasturbine. The gasturbine has a nominal speed of 500 000 rpm, a nominal air flow of 20 g/s and a nominal pressure ratio of 3. The compressor is tested in a turbo-shaft setup containing compressor, turbine, dummy generator and air bearings. The previously obtained results were limited to a test speed of 261 000 rpm due to instability of the conical whirling mode. For this reason, the compressor is now tested in a new rotor-bearing configuration with a dummy generator and two aerodynamic journal bearings with a flexible, damped support.

## ROTOR-BEARING CONFIGURATION

### Rotor layout

The previous rotor-bearing configuration is shown in figure 1 (top) and consists of one aerostatic journal bearing and two aerostatic thrust bearings. The tilt stiffness is predominantly generated by the two thrust bearings. With this configuration, the test speed was limited by a conical whirling instability which became apparent at 261 000 rpm. The close agreement between the numerically and experimentally obtained compressor performance, as reported last year [1], motivated us to test the compressor in a new rotor-bearing configuration with an improved stability behaviour.

Figure 1 (bottom) depicts the newly proposed rotor-bearing configuration with a dummy generator. The rotor is supported by two aerodynamic journal bearings located respectively in between compressor and turbine and at the left side of the dummy generator. The journal bearings are of the aerodynamic type and are stabilised by means of a flexible, damped support as described in [2,3]. The proven superior stability characteristics of these bearings should guarantee stable operation up to and beyond the design speed of 500 000 rpm. The thrust bearings are of the aerostatic type, thus very similar to the ones in the previous layout.

### Journal bearings with a flexible, damped support

Both journal bearings consist of a non-rotating bearing bush which is flexibly supported with respect to the bearing housing. The bearing bush has a self-acting wave-shaped height profile (diameter 8 mm, slenderness ratio 1) on its inner side which combines load-generating capability with favourable intrinsic stability properties [2]. On the outside, the bearing bush is supported by a flexible structure providing both stiffness and damping. Additional damping is provided by an oil squeeze film damper, of which the damping can be tuned by varying the oil viscosity.

### Effect on rotor dynamics

The new layout has the following consequences:

- The longer rotor has a higher mass, which lowers the stable operating speed (when other parameters

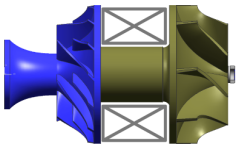

PREVIOUS LAYOUT:

- aerostatic journal bearing
- aerostatic thrust bearings
- 261 000 rpm due to conical instability

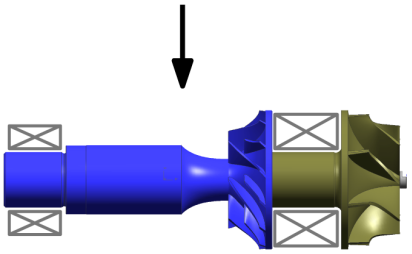

NEW LAYOUT:

- aerodynamic journal bearings with flexible, damped support
- aerostatic thrust bearings
- dummy generator

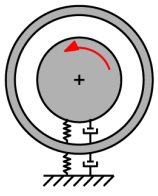

*Fig. 1: Old and new rotor-bearing layouts*

remain unchanged).

- The tilt stiffness originating from the two radial bearings is much higher than the contribution from the thrust bearings. As these radial bearings are well damped, the conical whirling mode – the speed limit for the previous layout – will be suppressed.
- The long slender shaft is now prone to centrifugal bending and therefore has to be balanced in three planes instead of two.
- Additional vibration modes are introduced by the suspended bearing bushes.

**Rotor dynamic model**

A rotor dynamic model is constructed incorporating (1) speed and frequency dependent bearing characteristics, (2) geometry and mass of the rotor, (3) mass, support stiffness and damping for the bearing bushes. Bending modes of the shaft are not taken into account. The model gives as output the eigenmodes with corresponding eigenfrequencies and damping ratios, as a function of rotor speed. Figure 2 shows that for the new rotor-bearing configuration, all modes have negative damping ratios over the whole speed range up to 600 000 rpm (10 kHz). This predicts stable operation over the whole operating range.

It is important to notice that all modes, whether they are (predominantly) conical or cylindrical, benefit from the damping in the radial bearings, and as such no damping is required in the thrust bearings, which greatly simplifies bearing construction.

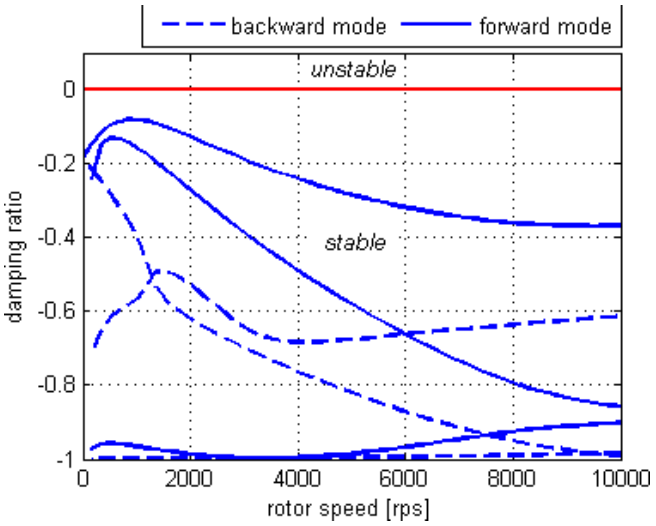


*Fig. 2: Prediction of the stability for the new rotor-bearing configuration.*

## PROTOTYPE AND TEST SETUP

The assembled rotor prototype is shown in figure 3. The left part consisting of compressor, dummy generator and bearing shaft is made from a single piece of titanium alloy (Ti6Al4V) by a combination of turning and 5-axis milling. The measurement surfaces for the optical probes are finished by diamond turning. To avoid seizing of the aerodynamic bearing during startup and coast down, a hardened steel ring is pressed over the bearing shaft. The turbine is made from $Si_3N_4$-TiN ceramic composite by spark erosion and grinding. The bearing stators are made from bronze by turning, milling and spark erosion.

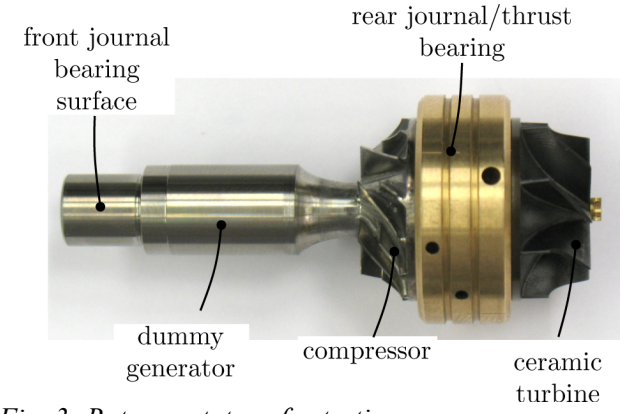


*Fig. 3: Rotor prototype for testing.*

The layout of the complete turboshaft setup is shown in figure 4. The rotor and bearings are mounted in a housing which consists of a compressor volute, and turbine volute, stator vanes and diffuser. Rotor whirling is monitored with three fiberoptic probes and a keyphasor. Two probes are located at the extremities of the rotor to measure its rigid body motions. The probe located in the centre detects bending of the shaft due to centrifugal forces acting on the remaining imbalance. To measure the performance of compressor and turbine, pressure and flow rate sensors are located at both compressor and turbine side.

## EXPERIMENTAL RESULTS

**Characterisation of the bearing support**

The static stiffness of the bearing support is measured without oil in the squeeze film damper. Figure 5 shows considerable hysteresis already present in the support structure, originating from dry friction.

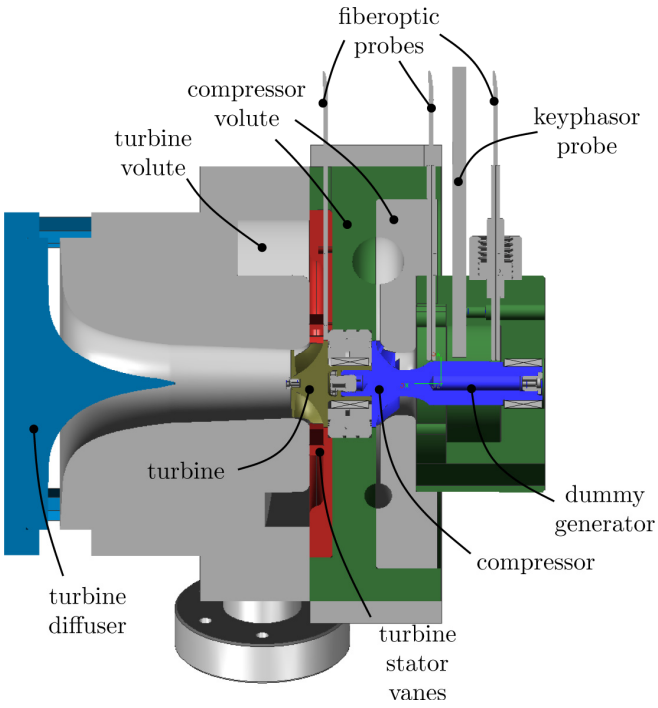


*Fig. 4: Layout of the instrumented setup.*

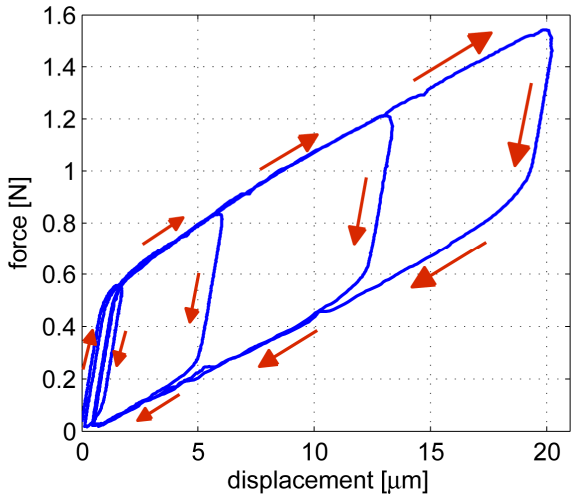


*Fig. 5: Stiffness characteristic of bearing support.*

**Balancing experiments**

Balancing of the rotor was done in situ by means of small balancing weights mounted on both ends of the rotor, more specifically in the hollow shaft of the front journal bearing and at the turbine end. From the size and (identical) orientation of the balancing weights, it was clear that the imbalance was mainly located at the compressor, probably due to a small misalignment of the pre-turned rotor in the 5-axis milling machine. The compressor imbalance combined with the balancing weights at the ends and in opposite direction of the compressor imbalance, generated a bending torque on the shaft. This was sufficiently reduced by balancing in a third plane located at the compressor rim: a small slot was milled in the compressor rim. Next, the rotor was rebalanced with smaller weights.

**Runup experiment**

Figure 6 shows the rotor whirling amplitude as a function of rotor speed, recorded during a runup experiment for the three channels (top), and the extracted conical and cylindrical whirling amplitudes (bottom). Critical speeds are encountered at 555 Hz and 710 Hz for respectively the cylindrical and conical whirls. Damping at these frequencies is low because the bearing stiffness at these rotational frequencies is low in comparison to the support stiffness and as a result the vibrations are not well transmitted to the damping structure. Nevertheless, these whirls occur at low speed and can therefore be passed safely during startup and coast down. At higher speeds, the vibration amplitudes increase again but level off towards asymptotic values as the rotor finally rotates around its centre of gravity.

The waterfall diagram in figure 7 shows a prominent synchronous vibration, excited by rotor imbalance, going through a peak around the previously mentioned critical speeds. There are also two self-excited whirls corresponding to the same conical and cylindrical modes, but now excited by bearing action. Thanks to the external damping, these self-excited whirls do not become unstable at higher rotational frequencies. The other lines on the waterfall diagram are measurement artefacts as explained in [3].

**Verification of compressor performance**

During the compressor performance tests, the turbine is driven with pressurised air, while the compressor load is varied. A compressor map is constructed as shown in figure 8, plotting pressure build-up against mass flow for different rotor speeds.

The data is measured and plotted along constant speed lines. A speed is selected by controlling the turbine supply. The different data points along the lines of constant speed are obtained by varying the compressor load. As power consumption of the compressor changes with load, the turbine supply has to be slightly adjusted to keep speed constant.

Both numerical and measured characteristics are plotted on the same graph. Numerical results are given for speeds up to 500 krpm which is the nominal speed of the system. Measured results are given for speeds up to 240 krpm (4 kHz). Measurements are not at exactly the same speed as the theoretical curves, and therefore 2 measured curves are slightly extrapolated to the speed of the neighbouring theoretical curve: 240 krpm extrapolated to 250 krpm, and 210 krpm extrapolated to 200 krpm. For extrapolation, pressure is assumed to vary quadratically with speed, while mass flow is assumed to vary linearly with speed.

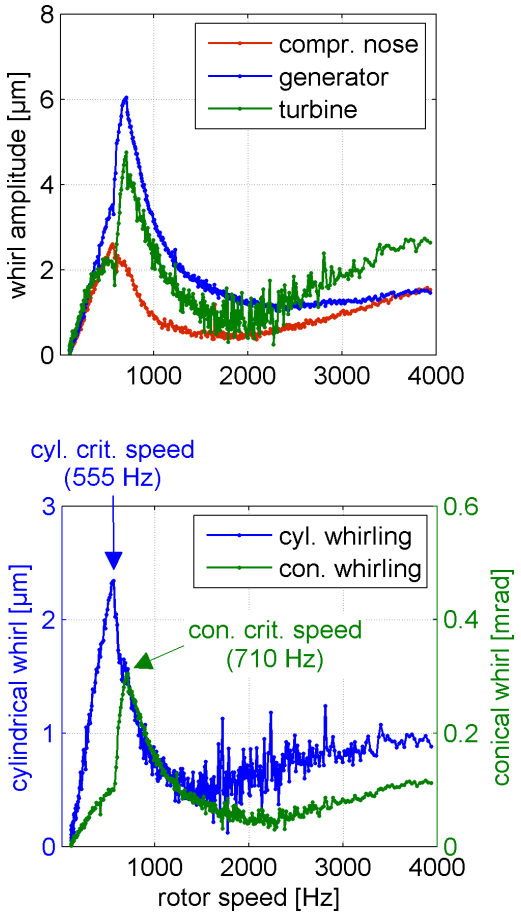


*Fig. 6: Rotor whirling during runup experiment.*

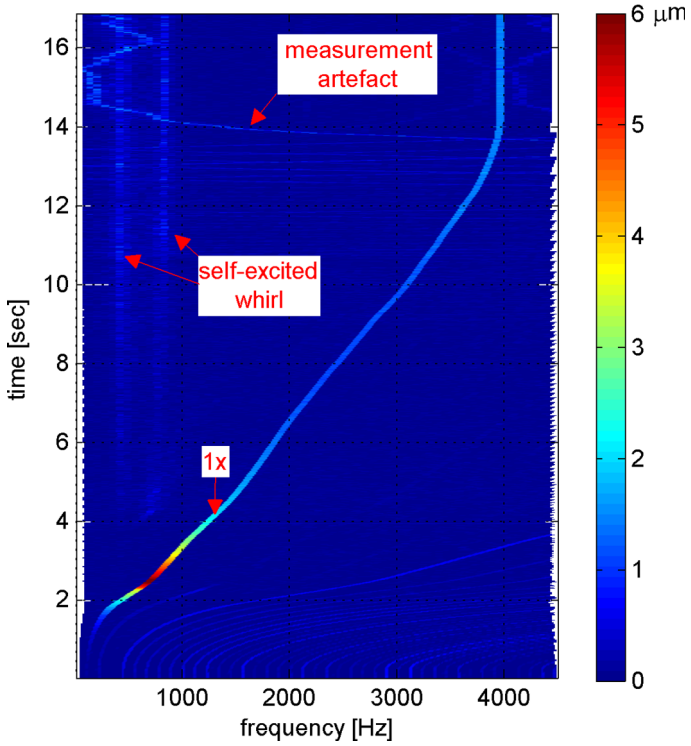


*Fig. 7: Waterfall diagram for runup experiment.*

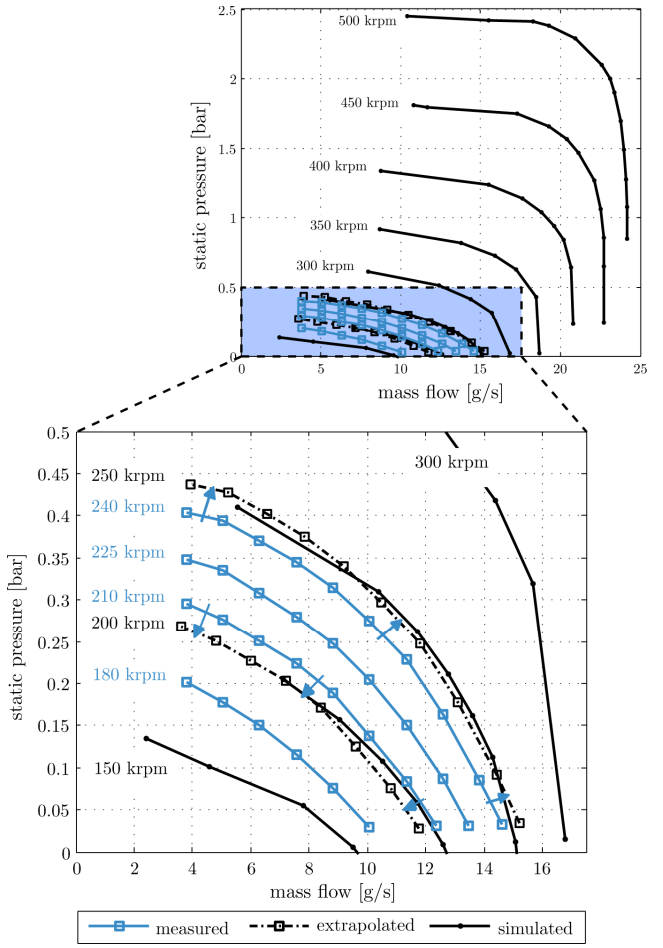


*Fig. 8: Comparison of measured and calculated compressor maps (pressure at diffuser exhaust).*

## DISCUSSION

Theoretical and measured results coincide very well, considering the uncertainty on the CFD calculations at low Reynolds numbers [4] (especially regarding the simple Baldwin-Lomax turbulence model) and the use of a tubular diffuser in the experimental setup as opposed to the annular diffuser in the numerical model. As the compressor is now operated at approximately half the nominal speed, the generated pressure is still low (0.41 bar relative static pressure) due to the (more than) quadratic relationship with speed. Nevertheless the good agreement between numerical and measured results suggests that the target pressure ratio will be attained at nominal speed.

## CONCLUSION

The new rotor-bearing geometry with externally damped bearings can successfully overcome rotor instability at high speed: the self-excited whirls are damped away. The remaining imbalance is smaller than the air bearing clearance. Therefore, the target speed of 500 krpm can now be reached.

The compressor performance was measured for speeds up to 4 kHz, showing a relative static pressure of 0.41 bar. The good agreement between numerical and measured results in the lower speed range suggests that the target pressure ratio will be attained at nominal speed.

## REFERENCES

[1] Peirs J, Waumans T, Liu K, Ferraris E, Verstraete T, Van den Braembussche R, Reynaerts D, 2009 Experimental verification of compressor performance for an ultra-microgasturbine, *Technical Digest PowerMEMS 2009 (Washington DC, USA, December 2009)* 92-95.

[2] Waumans T, Peirs J, Al-Bender F, Reynaerts D 2009 Design, optimisation and testing of a high-speed aerodynamic journal bearing with a flexible, damped support, *Technical Digest PowerMEMS 2009 (Washington DC, USA, December 2009)* 83-86.

[3] Waumans T, Peirs J, Al-Bender F, Reynaerts D Aerodynamic journal bearing with a flexible, damped support operating at 7.2 million DN, *Technical Digest PowerMEMS 2010 (Leuven, Belgium, December 2010)*.

[4] Verstraete T, Alsalihi Z, Van den Braembussche R A 2007 Multidisciplinary optimization of a radial compressor for micro gas turbine applications *ASME Turbo Expo 2007*, GT2007-27484, 9 pages.